Photodecomposition Kinetics of Formic Acid in Aqueous Solution

TAKESHI MATSUURA and J. M. SMITH

University of California, Davis, California

The photodecomposition of aqueous solutions of formic acid was studied as a model reaction for removing organic pollutants from water. The process was carried out in a tubular-flow reactor, operated continuously. The cylindrical reactor was irradiated from the outside by placing the cylindrical lamp and the reactor at the foci of an elliptical reflector. Measurements made at differential operating conditions permitted calculation of rates of reaction as a function of formic acid concentration and light intensity for the temperature range 25° to 60°C. Carbon dioxide and carbon monoxide were the only observed products of the decomposition.

The rate was first order in absorbed light intensity and between zero and first order in formic acid. These results correspond to a combination of chain and non-chain kinetics occurring simultaneously. Rate constant ratios and quantum yields were calculated from the data and the kinetics model.

A few measurements were made by adding ferric chloride and ferrous chloride to the feed to the reactor. An order of magnitude increase in rate was observed with these sensitizers.

The seriousness of water pollution (*1*) requires intensive study to develop efficient and economical methods of purification. The photochemical route may be a promising method, particularly for removal of residual or resistant compounds not decomposed by other processes.

Quantitative rate constants for photolysis of organic substances in water are unavailable, particularly values obtained in flow reactors which could be used with confidence for process development. The objective of the work reported here was to obtain rate constants, based upon a reasonable kinetics model, for a well-defined system, the photodecomposition of formic acid. This reaction is of interest in pollution studies because formic acid is toxic to aquatic life (*2*). Also the reaction is simple; only carbon dioxide and carbon monoxide need be determined in the product stream to follow the progress of the reaction. Measurements were made at acid concentrations from 0.01 to 0.44 g.-mole/liter and from 25° to 60°C. using a tubular-flow reactor irradiated with ultraviolet light of known intensity distribution with wavelength. The system was operated as a differential reactor (maximum conversion 0.25%) so that rates of reaction could be calculated from the measurements. Some data were also obtained to evaluate the catalytic effect of ferric and ferrous ions, added as sensitizers.

Photochemical means for decomposing organic pollutants have only recently been studied, and these results have not been obtained with the objective of extracting values of rate constants. Buller and Edgerley (*3*) irradiated vessels containing solutions of aldrin, dieldrin, and endrin and evaluated the extent of decomposition as a function of time and depth of solution (in the direction of radiation). Meiners and colleagues (*4*) applied radiation to a batch reactor and studied the extent of oxidation of starch by chlorine. Nonaka (*5*) measured the amount of decomposition of a linear alkyl benzene sulfonate (LAS) when treated with hydrogen peroxide alone and in the presence of radiation. The objective was to see if radiation reduced the foaming of the hydrogen peroxide-LAS system.

EQUIPMENT AND PROCEDURE

The reactor and accessories are shown in Figure 1. Formic acid solution flowed from reservoir 7, through reactor 9, and into stripping column 11. The liquid product was collected in flask 12 at the bottom of the column. To vary the oxygen content of the aqueous feed, provisions were available to saturate reservoir 7 with air, oxygen, or nitrogen. After steady state was reached, liquid samples for analysis were taken through sample line 10.

The stripping column, 1.05 cm. I.D. Pyrex tubing, 128 cm. long, was packed with glass beads. The effluent solution from the reactor was introduced at a location 28 cm. from the top of the column. Helium was introduced into flask 12 at the bottom of the separator. The stripped gases leaving the top of the column

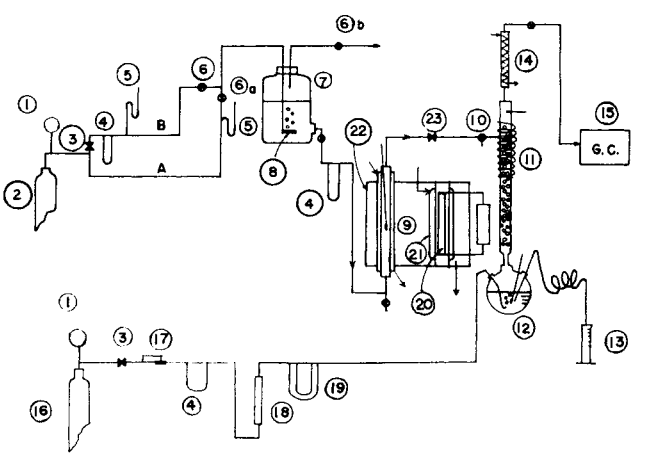

Fig. 1. Schematic diagram of equipment. (*1*) Pressure regulator. (*2*) O_2, N_2 cylinders. (*3*)Flow controller. (*4*) Capillary flowmeter. (*5*) Mercury manometer. (*6*) 6a, 6b Stopcocks. (*7*) Feed reservoir. (*8*) Gas distributor. (*9*) Reactor. (*10*) Three-way stopcock. (*11*) Gas-liquid separator. (*12*) Three-neck flask. (*13*) Graduated cylinder. (*14*) Liebig condenser. (*15*) Gas chromatograph. (*16*) He cylinder. (*17*) Flow regulator. (*18*) Soap filmmeter. (*19*) Silicagel drier. (*20*) Lamp. (*21*) Filter solution jackets. (*22*) Elliptical reflector. (*23*) Liquid flow controller.

passed through condenser 14, in which water was removed, and then were divided into two streams for analysis in the gas chromatograph 15. One stream was sent to column A (20 ft. of 5A molecular sieve, 30–60 mesh) for determination of oxygen, nitrogen, and carbon monoxide. In column B (10 ft. of Poropak Q from Varian Aerograph Co., 80–100 mesh) the second stream was analyzed for CO_2. Samples of the liquid feed and effluent were analyzed for formic acid by titration with sodium hydroxide solution.

The photoreactor system 9, 20, 22 was of the elliptical-reflector type, with reactor and lamp located at the foci of the ellipse. This type of system has been described in detail earlier (*6*). For the present work with a liquid feed, a reactor (of fused, optically clear quartz) 20 mm. I.D., 23 mm. O.D., and irradiated length of 200 mm., was employed. The temperature was held constant (±1°C.) by distilled water flowing at a controlled temperature through a jacket surrounding the reactor. The flow was always in the streamline regime ($Re = 4$ for final data). An entrance region of $L/D = 15$ was provided before the irradiated section, although this is not of significance for differential reactor operation (*9*).

A Hanovia (LL, 189A10, 1,200-w.) mercury-vapor lamp. 12, was the source of radiation. The spectrum of the energy output in the 2,000 to 3,500 Å. range, as supplied by the manufacturer (*7*), is given in the second column of Table 1.* The total light intensity was changed, with a minimum of variation in its spectral distribution, by circulating filter solutions at controlled temperatures through quartz jackets, 21, surrounding the lamp. These jackets, not shown separately in Figure 1, were formed by concentric quartz tubes whose I.D.-O.D. measurements were 42–45, 57–61, 70–74, and 85–89 mm. Through the annular space between the lamp and the first tube, air at room temperature was passed to cool the lamp. Distilled water was pumped through the second jacket, and through the third flowed solutions of $FeCl_3 \cdot 6H_2O$, adjusted to a *p*H of 1.8 with HCl. The walls of the outer jacket were carefully washed to remove contaminants which might absorb light. The annular space of this jacket contained air. Different intensity levels at the reactor wall were achieved by varying the concentration of $FeCl_3 \cdot 6H_2O$ circulated through the third jacket. These solutions and their concentrations were: filter solution #1, 0 g.-mole/liter; #2, 1.24×10^{-4}; #3, 2.45; #4, 4.96; #5, 7.38×10^{-4} g.-mole/liter; An initial radiation period is required to obtain stable transmission coefficients for the solutions. Checks on stability were made at intervals with a Beckman DK-2A spectrophotometer.

When runs with $FeCl_3$ as a sensitizer were made, the ferric ion concentration was determined by first reducing to Fe^{++} by titration with permanganate solution (*8*).

Light intensity was measured using the sensitized decomposition of oxalic acid as an actinometer solution passed through the same reactor. The feed solution contained uranyl sulfate, 0.001 molal, as sensitizer and oxalic acid in 0.005 molal concentration. This type of in-place actinometry is similar to that described in detail in earlier work (*9*).

PRELIMINARY EXPERIMENTAL STUDIES

Exploratory runs were made to evaluate reproducibility, effect of oxygen concentration in the feed solution, and limits of operating conditions for the stripping column.

Initial runs made over a two-day period at 26°C., feed rate of 7.2 cc./min., and feed concentration of HCOOH = 0.0871 g.-mole/liter produced carbon dioxide and carbon monoxide but not hydrogen in detectable concentrations. The conversion to carbon dioxide was 0.0883% and to carbon monoxide 0.0147%. The rates of carbon dioxide and carbon monoxide formation varied no more than ±3.5% during the period of the run. It has been suggested (*10*) that the overall reactions of aqueous solutions of HCOOH are

$$HCOOH + h\nu \longrightarrow H_2 + CO_2 \quad (1)$$

$$HCOOH + h\nu \longrightarrow H_2O + CO \quad (2)$$

and that these are followed by

$$HCOOH + H_2 \longrightarrow H_2O + HCHO \quad (3)$$

This secondary reaction is believed to explain the absence of detectable hydrogen among the products. The total rate of decomposition of HCOOH is given by the sum of the rates of formation of carbon dioxide and carbon monoxide:

$$\bar{\Omega}_d = \bar{\Omega}_{CO_2} + \bar{\Omega}_{CO} \quad (4)$$

The rates of formation of carbon dioxide and carbon monoxide were calculated from the flow rate Q and concentrations C_i in the product stream according to the equation

$$\bar{\Omega} = \frac{Q(C_i - 0)}{V} \quad (5)$$

In preliminary runs at constant feed composition Q was varied from 7.0 to 34.3 cc./min. and the helium rate to the stripping column from 24.5 to 85.4 cc./min. (at 26°C., atmospheric pressure). The rates calculated from Equation (4) were constant to ±4%, as long as the ratio of helium to feed flow rates was above 5.0. At lower ratios the rate of carbon dioxide formation decreased, suggesting incomplete removal from the liquid phase in the stripping column. The final data were taken with $Q = 7.2$ cc./min. and a helium rate of 43 cc./min. A further check on the stripping efficiency of the column was made by feeding water saturated with carbon dioxide from the reservoir and not radiating the reactor. Saturation conditions were 24°C. and atmospheric pressure. For a helium to water feed rate ratio of 6.0, the carbon dioxide measured in the helium from the stripping column was 0.788 cc. (at 0°C., 1 atm.) per cc. of water. This corresponds well with the reported solubility (*11*) at these conditions, 0.781 cc. of carbon dioxide per cc. of water.

Oxygen has been reported (*12*) to be an efficient free-radical scavenger, and thus to alter the course and rate of photochemical reactions. To test the possible effect of oxygen at the concentrations existing in the feed solution, experiments were carried out at two concentrations. In one case nitrogen was bubbled through the HCOOH feed solution (measured oxygen concentration = 4.5 p.p.m.), and in the second the feed was saturated with oxygen (measured oxygen concentration = 37.1 p.p.m.). In runs at 25°C. and at a feed rate and composition of 7.2 cc./min. and 0.0103 g.-mole/liter, the measured conversion to carbon dioxide was 0.20% for both conditions. It was concluded that oxygen at these low concentrations did not affect the decomposition. The final data were obtained using feed solutions through which nitrogen had been bubbled. Measured oxygen concentrations did not exceed 5 p.p.m.

Illustrative rate data obtained at the described conditions are shown in Figure 2 as a function of HCOOH concentration in the feed.

ANALYSIS OF DATA

Light Distribution in Reactor

The rate of a photoreaction depends upon the light intensity, and the intensity varies in the direction of the light path because of absorption. To analyze data from a photoreactor it is necessary to know the distribution of intensity. In the apparatus shown in Figure 1, the intensity is uniform along the length of the reactor, so the problem is one of evaluating the radial distribution of light across the diameter. Two extreme models have been used (*6*, *9*), both of which are idealized concepts. In one it is assumed that radially incident light of uniform intensity exists all around the reactor wall. Then the radial distribution within the reactor for uniform absorbent concentration is given by the integration of the Lambert-Beer relationship:

$$I_\lambda(r) = I_{\lambda,w} \frac{R}{r} \{\exp[-\mu_\lambda(R - r)] + \exp[-\mu_\lambda(R + r)]\} \quad (6)$$

*Material has been deposited as document 01202 with the ASIS National Auxiliary Publications Service, c/o CCM Information Sciences, Inc., 22 W. 34th St., New York 1001 and may be obtained for $2.00 for microfiche or $5.00 for photocopies.

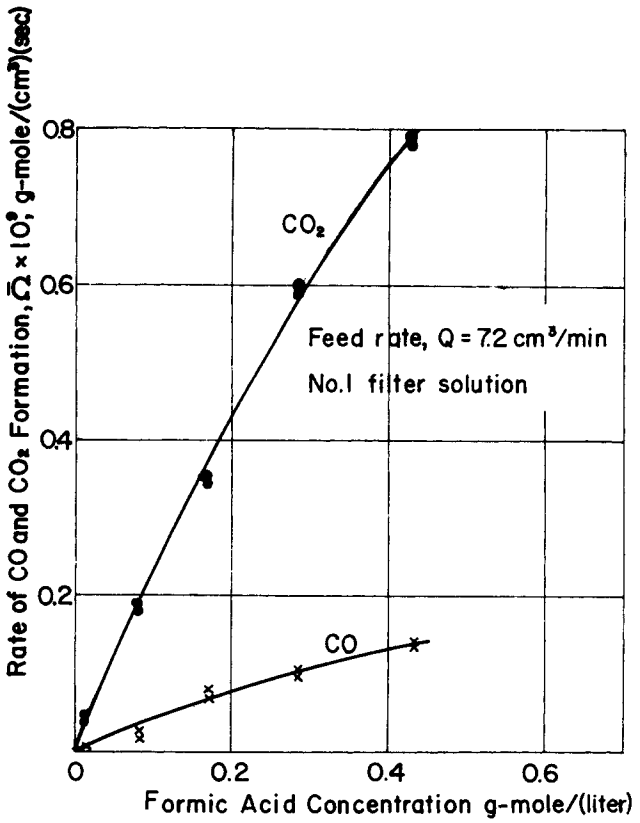

Fig. 2. Reaction rate versus formic acid concentration.

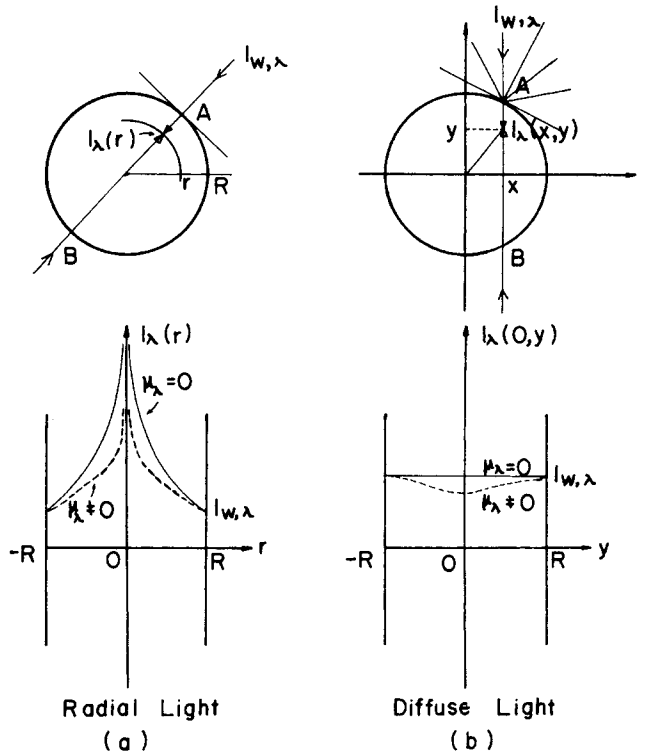

Fig. 3. Distribution of intensity within the reactor.

When the absorption due to reaction is negligible ($\mu_\lambda \longrightarrow 0$), Equation (6) reduces to

$$I_\lambda(r) = I_{\lambda,w}\frac{2R}{r} \tag{7}$$

Light profiles for $\mu_\lambda = 0$ and $\mu_\lambda \neq 0$ for this model are sketched in Figure 3*a*.

In the second model (diffuse light) it is supposed that there is equal probability for light from any direction to strike the reactor wall. It is also assumed that the light rays lie within planes normal to the reactor axis, as indicated in Figure 3*b*. If the single ray parallel to the y axis (AB in Figure 3*b*) is considered, the intensity at point (x, y) is given by Lambert-Beer's law:

$$I_\lambda^{AB}(x,y) = I_{\lambda,w}^{AB}\{\exp(-\mu_\lambda[(R^2-x^2)^{1/2}+y]) + \exp(-\mu_\lambda[(R^2-x^2)^{1/2}-y])\} \tag{8}$$

where $I_{\lambda,w}^{AB}$ is the intensity at the reactor wall due to ray AB. For light rays from any other direction, the intensity distribution will be the same as Equation (8), provided that the y coordinate is rotated to coincide with the direction of the ray. The same result would be obtained by rotating the light ray, rather than the y coordinate. If it is imagined that the rays from all directions are so rotated, the total intensity distribution will be, from Equation (8)

$$I_\lambda(x,y) = I_{\lambda,w}\{\exp(-\mu_\lambda[(R^2-x^2)^{1/2}+y]) + \exp(-\mu_\lambda[(R^2-x^2)^{1/2}-y])\} \tag{8a}$$

where $I_{\lambda,w}$ is the light intensity at the wall summed for rays from all directions. The intensity distribution given by Equation (8*a*) is an imaginary one and different from the actual intensity distribution which would be a function only of radius r. However, both distributions are based upon light rays from all directions. When the average reaction rate is calculated, by coupling either Equation (8*a*) or the actual distribution function with the rate equation and integrating over the reactor cross section, the result will be the same, provided that the rate is first order in I. Hence Equation (8*a*) may be used for the intensity distribution for the diffuse light model. This conclusion is restricted to the case where the reactor possesses cylindrical symmetry, that is, symmetry with respect to rotation about an axis normal to the plane of incident light.

If $\mu_\lambda \longrightarrow 0$, Equation (8*a*) reduces to

$$I_\lambda(x,y) = 2I_{\lambda,w} \tag{9}$$

Intensity profiles along coordinate y are shown for this model in Figure 3*b*. The average intensity for the whole reactor is $4\,I_{\lambda,w}$ from Equation (7), and $2\,I_{\lambda,w}$ from Equation (9). For a given average light intensity, this means that the incident intensity $I_{\lambda,w}$ calculated from the diffuse light model is twice as large as that calculated from the radial model.

Local Rate (Kinetics Model)

The mechanism of photolysis of formic acid solutions has been studied in photochemical cells (*10*, *13*). From these works the primary and secondary reactions are postulated to be

Primary reactions:

$$HCOOH \xrightarrow{\varphi_1 Ia} HCOO\cdot + H\cdot \tag{10}$$

$$HCOOH \xrightarrow{\varphi_2 Ia} \cdot CHO + \cdot OH \tag{11}$$

Secondary reactions:

$$HCOO\cdot \xrightarrow{k_{12}} CO_2 + H\cdot \tag{12}$$

$$H\cdot + HCOOH \xrightarrow{k_{13}} H_2 + CO_2 + H\cdot \tag{13}$$

$$\cdot CHO \xrightarrow{k_{14}} CO + H \cdot \qquad (14)$$

$$H + HCOOH \xrightarrow{k_{15}} H_2O + CO + H \cdot \qquad (15)$$

$$H \cdot \xrightarrow{k_{16}} \text{inert end product} \qquad (16)$$

Reactions (12) to (15) form chain cycles with H · as chain carrier. The termination situation is believed to be similar to that for photochlorination of propane (*9, 14*), that is, the termination of H · occurs by one or more first-order processes [represented by Equation (16)], either homogeneous with a scavenger, or heterogeneous, or both. In our work the reactor diameter is large and the diffusivity of H · in the liquid phase is likely to be small. Hence heterogeneous termination may not be very important. However, it is not necessary to neglect heterogeneous termination to arrive at the kinetics model.

From these elementary processes, a rate equation for the decomposition of HCOOH can be derived, provided the steady state hypothesis is valid. Using this approach the concentrations of intermediate species are

$$(HCOO \cdot) = \frac{\varphi_1 Ia}{k_{12}} \qquad (17)$$

$$(\cdot CHO) = \frac{\varphi_2 Ia}{k_{14}} \qquad (18)$$

$$(H \cdot) = \frac{1}{k_{16}}(2\varphi_1 + \varphi_2) Ia \qquad (19)$$

Then from Equations (12) and (13) and (17) and (19) the total rate of carbon dioxide formation is

$$\Omega_{CO_2} = \varphi_1 Ia \left[1 + \frac{2k_{13}}{k_{16}}\left(1 + \frac{\varphi_2}{2\varphi_1}\right)(HCOOH)\right] \qquad (20)$$

Similarly, the total rate of formation of carbon monoxide from Equations (14) and (15) is

$$\Omega_{CO} = \varphi_2 Ia \left[1 + \frac{k_{15}}{k_{16}}\left(\frac{2\varphi_1}{\varphi_2} + 1\right)(HCOOH)\right] \qquad (21)$$

For monochromatic light $Ia = \alpha_\lambda I_\lambda C_A$ and α_λ represent the concentration and absorptivity of formic acid. Hence, for light of wavelength λ, Equations (20) and (21) may be written as

$$\Omega_{CO_2,\lambda} = \varphi_1(\alpha_\lambda I_\lambda C_A)\left[1 + \frac{2k_{13}}{k_{16}}\left(1 + \frac{\varphi_2}{2\varphi_1}\right)C_A\right] \qquad (22)$$

$$\Omega_{CO,\lambda} = \varphi_2(\alpha_\lambda I_\lambda C_A)\left[1 + \frac{k_{15}}{k_{16}}\left(\frac{2\varphi_1}{\varphi_2} + 1\right)C_A\right] \qquad (23)$$

The total rate of decomposition of HCOOH is, according to Equation (4), given by the sum of (22) and (23).

Both rate expressions contain zero and first-order terms (in brackets) in C_A. The former is associated with the nonchain mechanism according to Equations (12) and (14), and the first-order term is due to the chain mechanism of Equations (13) and (15). In photocell studies at 2,537 Å., Adams and Hart (*13*) found that the overall quantum yield for carbon dioxide, $\varphi(CO_2)$, was independent of C_A below 0.2 g.-mole/liter and increased as the formic acid concentration increased until $\varphi(CO_2) = 3.46$ at $C_A = 10$ g.-mole/liter. This indicates that the chain mechanism becomes significant at $C_A = 0.2$, although its rate is not large with respect to that of the nonchain mechanism. The date reported here were obtained in the transition range (that is, from 0.01 to 0.44 g.-mole/liter). Hence, both terms in Equations (22) and (23) should be significant for $C_A > 0.2$.

Average Rate in Reactor

For polychromatic light Equations (22) and (23) must be summed over λ. Assuming that the rate constants and φ are independent of λ, Equation (22) becomes

$$\Omega_{CO_2} = \varphi_1 C_A \left[1 + \frac{2k_{13}}{k_{16}}\left(1 + \frac{\varphi_2}{2\varphi_1}\right)C_A\right] \sum_\lambda \alpha_\lambda I_\lambda \qquad (24)$$

Differential reactor operation permits the calculation of an average rate by integrating Equation (24) over the cross-sectional area with C_A constant. If the radial light model [Equation (6)] is used, the average rate is

$$\bar{\Omega}_{CO_2} = \varphi_1 C_A \left[1 + \frac{2k_{13}}{k_{16}}\left(1 + \frac{\varphi_2}{2\varphi_1}\right)C_A\right] \times \frac{\sum_\lambda \alpha_\lambda I_{\lambda,w}}{\pi R^2} \int_0^R \frac{R}{r} \{\exp[-\mu_\lambda(R - r)] + \exp[-\mu_\lambda(R + r)]\} 2\pi r dr \qquad (25)$$

Since the light intensity level was varied only by introducing filter solutions, it is convenient to introduce a hypothetical intensity $I_{b,\lambda}$. This is the intensity which would exist at the reactor wall if no filter solutions were employed around the reactor. The total intensity for all wavelengths $I_{b,tot}$ is related to $I_{b,\lambda}$ by the normalized energy output of the lamp. Since this is known (see Table 1)

$$I_{b,\lambda} = I_{b,tot} \frac{F_\lambda}{F_{tot}} \qquad (26)$$

Then the wall intensity with filter solutions of transmission T_λ is given by

$$I_{\lambda,w} = I_{b,tot}\left(\frac{F_\lambda}{F_{tot}}\right) T_\lambda \qquad (27)$$

Substituting this expression in Equation (25) gives the rate of carbon dioxide formation in terms of the constant $I_{b,tot}$, the absorptivity α_λ of HCOOH, and the transmission of the filter solution

$$\bar{\Omega}_{CO_2} = \varphi_1 C_A \left[1 + \frac{2k_{13}}{k_{16}}\left(1 + \frac{\varphi_2}{2\varphi_1}\right)C_A\right] \times I_{b,tot} \sum_\lambda \left(\alpha_\lambda \frac{F_\lambda}{F_{tot}} T_\lambda\right) \times \frac{1}{\pi R^2} \int_0^R \frac{R}{r} \{\exp[-\mu_\lambda(R - r)] + \exp[-\mu_\lambda(R + r)]\} 2\pi r dr \qquad (28)$$

It is convenient for plotting graphs to express the experimental results in terms of a corrected rate, corresponding to no absorption of light; that is, a rate for $\mu_\lambda = 0$. This rate, from Equation (28), is

$$(\bar{\Omega}_{CO_2})_{corr} = 4\varphi_1 C_A \left[1 + \frac{2k_{13}}{k_{16}}\left(1 + \frac{\varphi_2}{2\varphi_1}\right)C_A\right] \times I_{b,tot} \sum_\lambda \left(\alpha_\lambda \frac{F_\lambda}{F_{tot}} T_\lambda\right) \qquad (29)$$

or

$$(\bar{\Omega}_{CO_2})_{corr} = f\bar{\Omega}_{CO_2} \qquad (30)$$

where

$$f = \frac{4\pi R^2 \sum_\lambda \alpha_\lambda \frac{F_\lambda}{F_{tot}} T_\lambda}{\sum_\lambda \alpha_\lambda \frac{F_\lambda}{F_{tot}} T_\lambda \int_0^R \frac{R}{r} \{\exp[-\mu_\lambda(R-r)] + \exp[-\mu_\lambda(R+r)]\} 2\pi r dr} \quad (31)$$

The correction factor f gives the magnitude of the effect of light attenuation on average rate. The experimental measurements give $\bar{\Omega}_{CO_2}$. This is converted to a corrected rate through Equation (30), using a correction factor f evaluated from Equation (31). Then, if the kinetics model is valid, the correct effect of light intensity and formic acid concentration on the rate is given by Equation (29).

Proceeding in an analogous way, the corrected rate for carbon monoxide formation is

$$(\bar{\Omega}_{CO})_{corr} = 4\varphi_2 C_A \left[1 + \frac{k_{15}}{k_{16}}\left(\frac{2\varphi_1}{\varphi_2} + 1\right) C_A\right] \times I_{b,tot} \sum \left(\alpha_\lambda \frac{F_\lambda}{F_{tot}} T_\lambda\right) \quad (32)$$

and $(\bar{\Omega}_{CO})_{corr}$ is evaluated from $\bar{\Omega}_{CO}$ using Equation (30) applied to carbon monoxide and Equation (31) for f.

If the diffuse light model [Equation (8)] is used, the expressions for the corrected rates are

$$(\bar{\Omega}_{CO_2})_{corr} = 2\varphi_1 C_A \left[1 + \frac{2k_{13}}{k_{16}}\left(1 + \frac{\varphi_2}{2\varphi_1}\right) C_A\right] \times I_{b,tot} \sum_\lambda \left(\alpha_\lambda \frac{F_\lambda}{F_{tot}} T_\lambda\right) \quad (33)$$

$$(\bar{\Omega}_{CO})_{corr} = 2\varphi_2 C_A \left[1 + \frac{k_{15}}{k_{16}}\left(\frac{2\varphi_1}{\varphi_2} + 1\right) C_A\right] \times I_{b,tot} \sum_\lambda \left(\alpha_\lambda \frac{F_\lambda}{F_{tot}} T_\lambda\right) \quad (34)$$

The corrected rates are evaluated from $\bar{\Omega}_{CO_2}$ and $\bar{\Omega}_{CO}$ using Equation (30), but now f is given by

$$f = \frac{2\pi R^2 \sum_\lambda \alpha_\lambda \frac{F_\lambda}{F_{tot}} T_\lambda}{\sum_\lambda \alpha_\lambda \frac{F_\lambda}{F_{tot}} T_\lambda \int_{-R}^{R} \int_{-(R^2-y^2)^{1/2}}^{(R^2-y^2)^{1/2}} \{\exp[-\mu_\lambda[(R^2-x^2)^{1/2} + y]] + \exp[-\mu_\lambda[(R^2-x^2)^{1/2} - y]]\} dx dy} \quad (35)$$

Equations (29) and (32) and (33) and (34) are to be compared with the experimental data. To evaluate the rate constants, the absolute level of light intensity ($I_{b,tot}$) must be determined. These measurements are summarized in the next section (Actinometry). However, the validity of the equations with respect to variations in intensity can be determined immediately.

Effect of Light Intensity

Since the lamp output and $I_{b,tot}$ were the same for all the runs, the effect of light intensity can be evaluated by the relation between the transmission of the filter solutions and the rates. According to Equations (29), (32), (33), or (34), the rate should be directly proportional to the summation of $\alpha_\lambda \frac{F_\lambda}{F_{tot}} T_\lambda$. The individual variables over the entire range of wavelength, and the summations for each filter solution, are reported in Table 1. The absorptivities for HCOOH shown in the table were measured with a Beckman DK-2 spectrophotometer. Values were determined at temperatures from 30° to 60°C., but varied little over this range. The results in the table are for 45°C. The values of f were calculated from Equations (31) and (35), using the data in Table 1. The results are given in Table 2 for various formic acid concentrations. Despite the differences in profiles (Figure 3), the correction factors are approximately the same for radial and diffuse light. Hence either light pattern can be used to relate the local and average rates, and the pattern employed will have no effect upon the comparison between the data and the kinetics model.

TABLE 2. CORRECTION FACTOR f

Filter solution No.	HCOOH Conc., g.-moles/cc. × 10^5	Correction factor f: Radial light [Eq. (31)]	Correction factor f: Diffuse light [Eq. (35)]
1	1.03	1.356	1.341
	8.75	3.555	3.336
	17.42	5.418	5.129
	28.82	7.394	7.151
	43.5	9.451	9.381
2	1.03	1.344	1.331
	8.75	3.388	3.193
	17.42	5.044	4.796
	28.82	6.746	6.541
	43.5	8.476	8.405
3	1.03	1.327	1.316
	8.75	3.172	3.006
	17.42	4.595	4.390
	28.82	6.008	5.841
	43.5	7.403	7.341
4	1.03	1.286	1.281
	8.75	2.694	2.591
	17.42	3.635	3.520
	28.82	4.491	4.406
	43.5	5.286	5.253
5	1.03	1.295	1.289
	8.75	2.657	2.572
	17.42	3.443	3.374
	28.82	4.089	4.064
	43.5	4.651	4.675

The corrected rates for carbon dioxide and carbon monoxide are shown in Figure 4 for both light patterns based upon data for C_A = 0.174 g.-mole/liter. The linear relationship between the rate and $\sum \left(\alpha_\lambda \frac{F_\lambda}{F_{tot}} T_\lambda\right)$ is observed. This indicates that the first-order dependency of rate upon $I_{\lambda,w}$, suggested by the kinetics model [for example, Equation (25)], is in agreement with the data.

ACTINOMETRY

The absolute light intensity, as $I_{b,tot}$, was determined by measuring the rate of decomposition of oxalic acid in uranyl sulfate solution. In a restricted concentration range

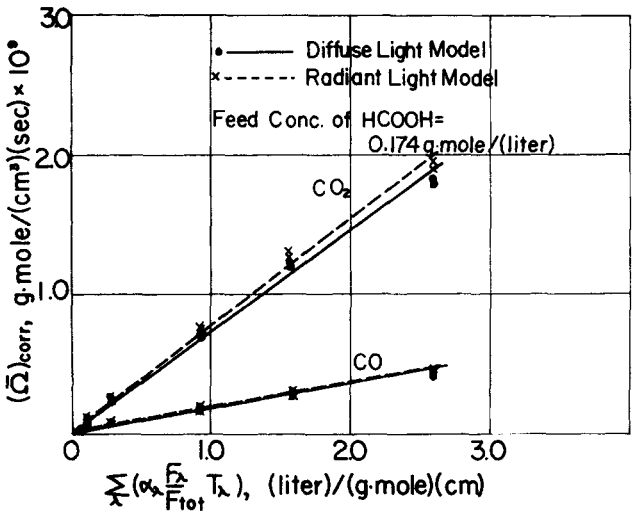

Fig. 4. Effect of light intensity on the rates.

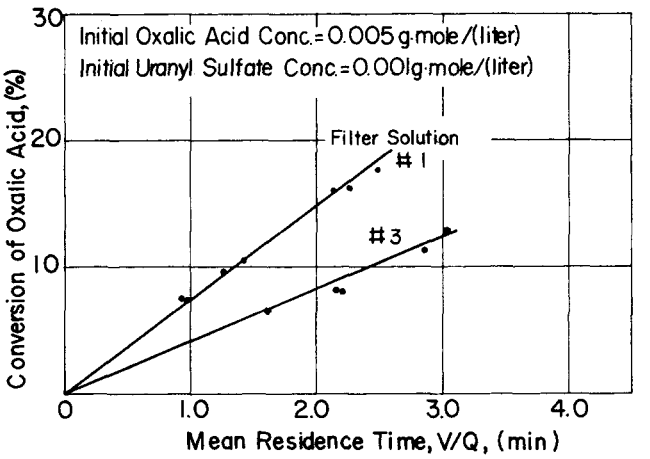

Fig. 5. Results of actinometer runs.

this reaction is zero order, so that the local rate is

$$r_\lambda = Ia_\lambda(\varphi_a)_\lambda = I_\lambda C\,\alpha_\lambda(\varphi_a)_\lambda \tag{36}$$

The absorptivity and quantum yield are well established (*15*), and tabulated for the appropriate wave length range for this work in Table 3*. The average rate can be obtained by using Equations (6) or (8) for I_λ and integrating across the diameter of the reactor. Since differential reactor conditions are maintained, C is essentially constant for this integration. The resultant equations for $\bar{r}$, developed in the same way as Equation (25), are

$$\bar{r} = \frac{I_{b,\text{tot}}}{\pi R^2} C \sum_\lambda (\varphi_a)_\lambda \alpha_\lambda \frac{F_\lambda}{F_{\text{tot}}} T_\lambda \int_0^R \frac{R}{r} \{\exp[-\mu_\lambda(R-r)] + \exp[-\mu_\lambda(R+r)]\}\, 2\pi r dr \tag{37}$$

for the radial light model, and

$$\bar{r} = \frac{I_{b,\text{tot}}}{\pi R^2} C \sum_\lambda (\varphi_a)_\lambda \varphi_\lambda \frac{F_\lambda}{F_{\text{tot}}} T_\lambda \times \int_{-R}^{R} \int_{-(R^2-y^2)^{1/2}}^{(R^2-y^2)^{1/2}} \{\exp[-\mu_\lambda[(R^2-x^2)^{1/2}+y]] + \exp[-\mu_\lambda[(R^2-x^2)^{1/2}-y]]\}\, dx dy \tag{38}$$

for diffuse light.

The measured conversions of oxalic acid can be converted to average rates of reaction $\bar{r}$ and then used in Equation (37) or (38) to evaluate $I_{b,\text{tot}}$, since all other quantities are known. Equation (5) applied to the actinometer case and written in terms of conversion becomes

$$\bar{r} = \frac{Q}{V}(C_0 - C) = \frac{Q}{V}(C_0)\,x \tag{39}$$

where x is the conversion of oxalic acid leaving the reactor.

The actinometer runs were made, after all the formic acid data were obtained, at two light intensities, corresponding to filter solutions 1 and 3, The values of $\sum\left(\alpha_\lambda \frac{F_\lambda}{F_{\text{tot}}} T_\lambda\right)_{act}$ for these two cases are given in Table 3. In all runs $t = 26°C$. Reproducible results could be obtained as long as the flow rate was greater than 20 cc./min. (corresponding to a Reynolds number of 11) and the conversion was less than 20%. The experimental results are shown in Figure 5 as conversion versus V/Q. The average rates calculated according to Equation (39) were 6.25×10^{-9} and 3.46×10^{-9} g.-mole/(cc.)(sec.) for filter solutions 1 and 3, respectively. Using these results and the data given in Table 3, $I_{b,\text{tot}}$ was calculated from Equations (37) and (38) for each filter solution. The results, shown in Table 4, differ by somewhat less than 5% and probably are a fair measure of the accuracy of the measurement of light intensity. Note that $I_{b,\text{tot}}$ is about twice as large for the diffuse light as for the radial light model, as mentioned earlier.

TABLE 4. TOTAL LIGHT INTENSITY $I_{b,\text{tot}}$, EINSTEINS/(SQ. CM.)(SEC.) × 10^9

	Filter solution 1	Filter solution 5	Average
Radiant light	11.38	10.92	11.15
Diffuse light	21.20	20.30	20.75

EVALUATION OF RATE CONSTANTS

Equation (29) can be rearranged to the form

$$\frac{(\bar{\Omega}_{CO_2})_{\text{corr}}}{C_A} = B_{CO_2} + B_{CO_2}\frac{2k_{13}}{k_{16}}\left(1 + \frac{\varphi_2}{2\varphi_1}\right)C_A \tag{39}$$

where

$$B_{CO_2} = 4\varphi_1 I_{b,\text{tot}} \sum_\lambda \left(\alpha_\lambda \frac{F_\lambda}{F_{\text{tot}}} T_\lambda\right) \tag{40}$$

It the kinetics model fits the data, a plot of the left side versus C_A should be a straight line. Similar rearrangement of Equation (32) suggests a linear plot of the carbon monoxide rate results, where the constant B_{CO} is the same as defined by Equation (40), except φ_2 replaces φ_1. In an analogous fashion, Equations (33) and (34) indicate that similar linear relationships should exist when the diffuse light model is employed. Figure 6 shows the data plotted in this way for both carbon dioxide and carbon monoxide, and for both light models. The experimental data were taken with filter solution 1. The experimental points do fit a linear relationship and lend confidence to the idea of both chain and nonchain mechanisms contributing to the rates.

*Material has been deposited as document 01202 with the ASIS National Auxiliary Publications Service, c/o CCM Information Sciences, Inc., 22 W. 34th St., New York 10001 and may be obtained for $2.00 for microfiche or $5.00 for photocopies.

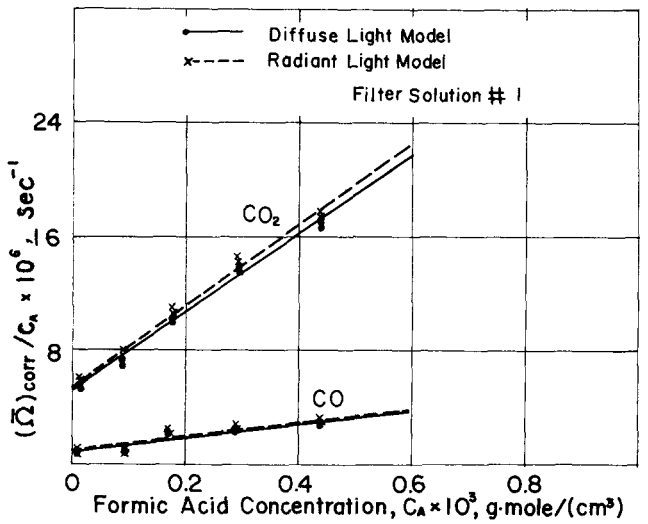

Fig. 6. Correlation of rate data versus C_A.

From the intercepts (B_{CO_2} values) in Figure 6, and known values for $I_{b,tot}$ in Table 4 and $\sum \left(\alpha_\lambda \frac{F_\lambda}{F_{tot}} T_\lambda\right)$ in Table 1, φ_1 can be calculated using Equation (40). In a similar way B_{CO} and φ_2 can be evaluated. The slopes of the lines in Figure 6 are functions of B and the rate constants; for example, the slope of the line for carbon dioxide is

$$\text{slope} = B_{CO_2} \frac{2k_{13}}{k_{16}} \left(1 + \frac{\varphi_2}{2\varphi_1}\right) \tag{41}$$

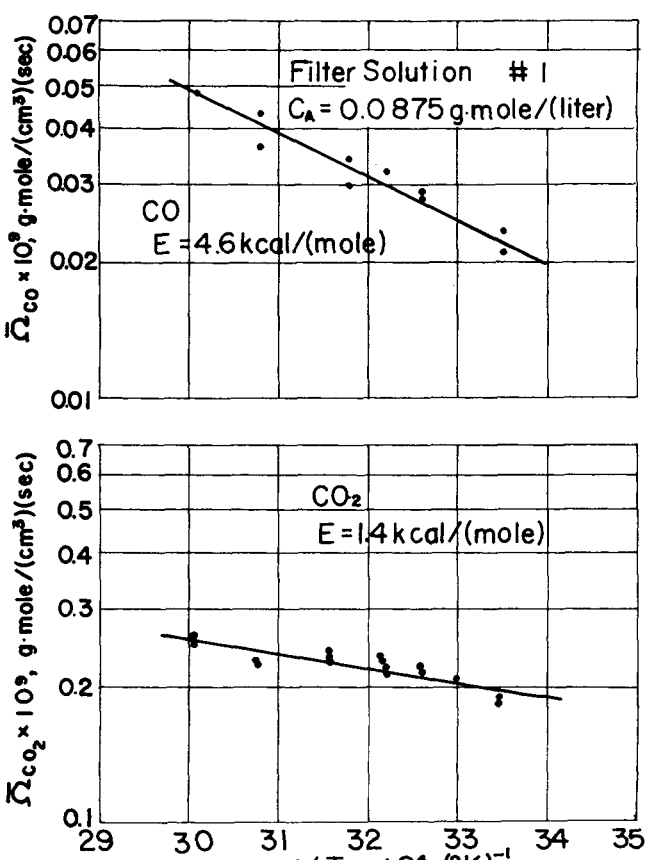

Fig. 7. Temperature effect on rates of carbon dioxide and carbon monoxide formation.

Table 5. Quantum Yields and Rate Constants

	φ_1 (for HCOO·) g.-mole/ Einstein	φ_2 (·CHO) g.-mole/ Einstein	k_{13}/k_{16} cc./ g.-mole	k_{15}/k_{16} cc./ g.-mole
Radial light	0.0466	0.0086	2.54×10^3	0.41×10^3
Diffuse light	0.0483	0.0093	2.44×10^3	0.42×10^3

Since B_{CO_2}, φ_1 and φ_2 are already known, the ratio k_{13}/k_{16} can be calculated. Similarly, k_{15}/k_{16} is established from the carbon monoxide data. The results are summarized in Table 5. Radial and diffuse light patterns give nearly the same results. The values for φ_1 and φ_2 are about 10% of those measured in photocells using monochromatic light; that is, $\varphi_1 = 0.48$ and $\varphi_2 = 0.14$ at 2,537 Å. and C_A = 0.1 g.-mole/liter as measured by Adams and Hart (*13*). The lower values in Table 5 are likely due to the opacity of quartz and incomplete reflection of the ellipsoidal, aluminum reflector at wavelengths below 2,500 Å. The most intense absorption of light by HCOOH occurs in this region.

Rates of carbon dioxide and carbon monoxide formation were measured at $C_A = 0.0875$ g.-mole/liter using filter solution 1 (distilled water) over the temperature range 25° to 60°C. The Arrhenius plots of the data (Figure 7) indicate overall activation energies of 1.4 and 4.6 kcal./g.-mole for carbon dioxide and carbon monoxide, respectively. These small values are the normal expectancy for photochemical reactions.

PHOTOSENSITIZED DECOMPOSITION OF HCOOH

The previous results show that the rate of decomposition of formic acid by photolysis is very low; conversions were always less than 0.25% at residence times up to 500 sec. As a means of increasing the rate, ferric and ferrous ions were added as $FeCl_3$ and $FeCl_2$. Also the effect of dissolving oxygen in the formic acid was studied. The results are summarized in Table 6. All data are at 26°C., with filter solution 1 (distilled water) and at about 500 sec. average residence time in the reactor. The initial HCOOH concentration was about 0.011 g.-mole/liter for all runs. Runs *A* and *B* were made with photosensitizers, but the initial oxygen concentration in *B* was increased. As mentioned earlier, oxygen has little effect on the rates. In run *C* ferric chloride was added, and the rate of carbon dioxide formation was 62 times as large as in *A*. Run *D* is a duplicate of *C* except that the oxygen concentration has been increased. The rate of carbon dioxide formation increased somewhat further, and the oxygen concentration decreased by 34% between product and feed streams. Apparently oxidative decomposition of HCOOH is induced not only by ferric ions

Table 6. Photosensitization Results

Run	A	B	C	D	E
Feed concentration:					
Fe^{+++}, g.-mole/cc. $\times 10^6$	0	0	3.65	3.65	0
Fe^{++}, g.-mole/cc. $\times 10^6$	0	0	0	0	4.83
O_2, g.-mole/cc. $\times 10^7$	1.40	11.6	1.36	12.3	3.19
$\bar{\Omega}_{CO_2}$, g.-mole/(cc.)(sec.) $\times 10^9$	0.04	0.04	2.48	3.03	0.82
$\bar{\Omega}_{CO}$, g.-mole/(cc.)(sec.) $\times 10^9$	0.006	trace	0	0	trace
Decrease in O_2, conc., %	0	0	0	34	58
Product concentration:					
Fe^{+++}, g.-mole/cc. $\times 10^6$	0	0	1.57	2.20	2.71
Fe^{++}, g.-mole/cc. $\times 10^6$	0	0	2.08	1.45	2.12
Conversion of HCOOH, %	0.2	0.17	10.7	13.2	3.6

but by molecular oxygen. In run E, $FeCl_2$ was substituted for $FeCl_3$. In this case oxygen was consumed and also ferrous ion was oxidized to ferric. The rate of carbon dioxide formation was less than when $FeCl_3$ was used, but it was still 20 times greater than that obtained without any sensitizer (run A).

The decomposition of HCOOH with $FeCl_3$ in the presence of solar light was studied by Benrath (*14*). From the products observed, the chief reaction was concluded to be

$$HCOOH + 2FeCl_3 \xrightarrow{h\nu} 2FeCl_2 + CO_2 + 2HCl \qquad (42)$$

The results of run C, in which carbon dioxide formation and simultaneous reduction of ferric to ferrous ion was observed, agree with this reaction. However, runs D and E, showing that $FeCl_2$ is an effective sensitizer, and is oxidized, suggest the following reaction:

$$2FeCl_2 + 2HCl + \frac{1}{2}O_2 \xrightarrow{h\nu} 2FeCl_3 + H_2O \qquad (43)$$

For these cases the overall process is given by the sum of Equations (42) and (43)

$$HCOOH + \frac{1}{2}O_2 \xrightarrow[Fe^{+++},Fe^{++}]{h\nu} CO_2 + H_2O \qquad (44)$$

Ferric and ferrous ions can be thought of as an oxidation-reduction catalyst rendered effective by ultraviolet light.

CONCLUSIONS

The local rate of formic acid photolysis was found to be first order in light absorbed and between zero and first order in formic acid concentration. Presumably this is due to the fact that both nonchain and chain mechanisms are important in part of the range of HCOOH concentration studied (0.01 to 0.44 g.-mole/liter). By using a kinetics model based upon these concepts, it was possible to correlate the rate data and evaluate quantum yields and ratios of rate constants.

Average rates were measured in the flow reactor, operated differentially. Therefore it was necessary to use a pattern for the light distribution in order to relate the measurements to the local rate. Two significantly different patterns, radial and diffuse light, were used. The quantum yields and ratios of rate constants were nearly the same for both models, suggesting that the relation between local and average rates is independent of light pattern. Care should be used in generalizing this result to other kinetics since HCOOH photolysis is first order in light absorbed.

Finally, it was found that ferric and ferrous ions act as a oxidation-reduction catalyst in the presence of ultraviolet light. With these photosensitizers present, the formic acid solution absorbs oxygen and HCOOH decomposes into water and carbon dioxide. These sensitizers increased the rate of decomposition by 20 to 60 times. Hence, they may be of interest in developing a photochemical process for removing organic pollutants from water.

ACKNOWLEDGMENT

The authors are grateful for the financial aid of the Federal Water Pollution Control Administration through Grant WP-00952.

NOTATION

C = oxalic acid concentration, g.-mole/cc.
C_0 = concentration in the feed stream
C_A = formic acid concentration, g.-mole/cc.
F_λ = energy output of lamp at wavelength λ, Einsteins/sec.
F_{tot} = total flux of lamp
f = correction factor as defined by Equations (31) and (35)
I_λ = light intensity at wavelength λ, Einsteins/(sq. cm.) (sec.)
I_w = intensity at reactor wall with filter solution
$I_{b,tot}$ = intensity which would exist at reactor wall if no filter solution were used
Ia = absorbed light of intensity I, Einsteins/cc.
k_i = reaction rate constants for elementary reaction i as defined by Equations (12) to (16)
Q = volumetric flow rate through reactor, cc./sec.
R = inside radius of the reactor, cm.
r = radial coordinate in reactor, cm.
r_λ = rate of oxalic acid decomposition at wavelength λ, g.-mole/(cc.) (sec.)
$\bar{r}$ = average rate over cross section of the reactor, summed for all wavelengths
T_λ = fraction of light, of wavelength λ, which is transmitted through the filter solution
V = irradiated volume of reactor, cc.
V/Q = average residence time
w = reactor wall
x, y = coordinates in diffuse light model (Figure 3*b*)

Greek Letters

α_λ = absorptivity. Data in tables are in units of liter/(g.-mole) (cm.); in equations units are sq. cm./g.-mole. All values are based upon the intensity ratio in $\log_e$ form
Ω_λ = reaction rate (CO_2 or CO) at wavelength λ, g.-mole/(sec.) (cc.)
Ω_d = total rate of decomposition of HCOOH
$\bar{\Omega}$ = average rate over cross-sectional area of reactor, summed for all wavelengths
$\bar{\Omega}_{corr}$ = corrected average rate as defined by Equation (30)
μ_λ = attenuation coefficient ($\mu_\lambda = \alpha_\lambda C_A$) at wavelength λ, cm.$^{-1}$
$(\varphi_a)_\lambda$ = quantum yield of oxalic acid decomposition at wavelength λ, g.-mole/Einstein
φ_1 = quantum yield of HCOO · formation [Equation (10)], g.-mole/Einstein
φ_2 = quantum yield of · CHO formation [Equation (11)], g.-mole/Einstein

LITERATURE CITED

1. Moore, J. C., *Chem. Eng.*, **75**, 18 (1968).
2. Ericksen, Jones, J. R., "Fish and River Pollution," Butterworth, London (1964).
3. Buller, C. D. III, and E. Edgerley, Jr., *J. Water Pollution Control Fed.*, **40**, 546 (1968).
4. Meiners, A. F., M. E. Whitehead, E. A. Lawler, and J. I. Morrison, paper presented at Am. Chem. Soc. Meeting, Water, Air and Waste Chem., Atlantic City, N. J. (September 1968).
5. Nonaka, D. N., M.S. thesis, Georgia Inst. Techn., Atlanta (August, 1968).
6. Matsuura, T., A. E. Cassano, and J. M. Smith, *AIChE J.*, **15**, 495 (1969).
7. Hanovia Lamp Co., *Bull. EH-223*.
8. Kolthoff, I. M., and E. B. Sandell, "Textbook of Quantitative Inorganic Analysis," American Co., New York (1936).
9. Cassano, A. E., and J. M. Smith, *AIChE J.*, **12**, 1124 (1966); **13**, 915 (1967).
10. Allmand, A. J., and L. Reeve, *J. Chem. Soc. 2852* (1926).
11. Hodgman, C. D., ed., "Handbook of Chemistry and Physics," 36 edit. (1945–55).
12. Calvert, J. G., and J. N. Pitts, Jr., "Photochemistry," Wiley, New York (1966).
13. Adams, G. E., and E. J. Hart, *J. Am. Chem. Soc.*, **84**, 3994 (1962).
14. Benrath, A., *J. Prakt. Chem.*, **72**, 220 (1905).
15. Bracket, F. P., Jr., and G. S. Forbes, *J. Am. Chem. Soc.*, **55**, 4459 (1933).

Manuscript received April 9, 1969; revision received June 5, 1969; paper accepted June 9, 1969.